

## A NOVEL LNG COLD ENERGY INTEGRATED UTILIZATION SYSTEM

Kang Chen<sup>1</sup>, Yang Du<sup>1</sup>, Yiping Dai<sup>1\*</sup>, Tianliang Yang<sup>2</sup>, Xiaowei Zheng<sup>2</sup>, Wenbin Li<sup>3</sup>

1. School of Energy and Power Engineering, Xi'an Jiaotong University, Xi'an, Shaanxi Province, China

2. Yantai Longyuan Power Technology CO. LTD, Yantai, Shandong Province, China

3. Qingdao Zhongji Longyuan Energy Technology CO. LTD, Qingdao, Shandong Province, China

\*Corresponding Author: Yiping Dai E-Mail address: ypdai@mail.xjtu.edu.cn

### ABSTRACT

Liquefied natural gas (LNG) contains abundant cold energy, which is of high grade. Reasonable recycling can help reduce energy loss, carbon emissions and contribute to the sustainable development of mankind. Aiming at the recovery and utilization of LNG cold energy, a new type of integrated system is proposed. By reasonably coupling the power generation system and the intermediate cold energy recovery system, the efficient cascade recovery and utilization of LNG cold energy can be realized. On this basis, the thermodynamic design and analysis of the cold energy power generation system in the integrated system are carried out, and the one-dimensional thermodynamic design of the two turbines in the power generation system is carried out according to the thermodynamic design results of the whole system. The results show that: the cold energy recovery rate of the power generation system is 22.74%, while the cold energy recovery rate is 33.24%. The power of the two turbines are 3952.577 kW and 2083.361 kW, respectively, and the isentropic efficiencies are 81.86% and 82.51%, respectively. The research results have certain guiding significance for practical engineering applications.

### 1 INTRODUCTION

With the acceleration of economic globalization and the modernization process, the demand for energy by mankind is increasing, and the environmental pollution brought by it has become more and more serious (**Global, B.P. 2011**). As one of the three major fossil energy sources, natural gas has large reserves and high calorific value. Its combustion process is cleaner and more efficient than coal and oil, which has less impact on the environment and is safe to use. In recent years, consumption of natural gas has steadily increased (**Soldo, B., 2012**). Liquefied natural gas (LNG) is a liquid that comes from the pressurized natural gas cooled to  $-162^{\circ}\text{C}$ . Its volume is 625 times smaller than conventional natural gas, and its density is only about 45% of the same volume of water (**Ikoku, C.U.1980**). Besides, the energy density of LNG is comparable to conventional gasoline, which is convenient for large-scale long-distance transportation and storage.

Without natural refrigeration, the production of LNG per ton requires about 850 kW·h of electricity (**Wong, W.1994**), and LNG cannot be used directly in a liquid state. It will release about 241kW·h of energy when LNG absorbs heat to become conventional natural gas. Generally, LNG receiving stations are built near the sea and use seawater as a heat source to heat LNG. On the one hand, in order to prevent the temperature of seawater from falling sharply and freezing, a large amount of seawater needs to be consumed for heating the LNG, but the low-temperature seawater produced directly discharged into the ocean without treatment will cause large-scale marine cold pollution, which will seriously affect the aquaculture industry and destroy the marine ecological balance (**Dubinsky, Z.V.Y.& Stambler, N. 1996**). On the other hand, the use of seawater to heat LNG will cause the high-grade low-temperature cold energy of LNG to be wasted, thereby aggravating the consumption of social resources. Therefore, it is necessary to reasonably recycle the cold energy of LNG.

The cold energy contained in LNG is of high grade and can be recovered and applied in many fields, And the main recovery methods include direct recovery and indirect recovery (**Hirakawa, S.& Kosugi, K 1981**). Researchers have proposed different solutions for different LNG cold energy recovery and utilization backgrounds. A comprehensive review on the state-of-the-art LNG cold energy utilization systems is provided by **He Tianbiao et.al (2018)**, and technologies to utilize LNG cold energy are analyzed and compared. **Bao Junjiang (2019)** et.al proposed power generation systems based on LNG cold energy in series and parallel, and the system parameters and working fluids are optimized simultaneously to discuss which combination method is better. **Ma Guoguang (2018)** et.al established

a novel multi-stage Rankine cycle for LNG cold-energy power generation system and studied the effect of gasification pressure and seawater temperature on the system performance. Besides, the principle of refrigerant selection in the Rankine cycle for LNG cold-energy power generation system is determined. **Li Chenghao (2019)** et.al introduced a solar heating system to enhance the outlet temperature of the working fluid that can improve the working capacity of the whole system. Results indicated that the thermal efficiency of the system could be enhanced to 28.32% through optimization, which is quite higher than the conventional power generation for LNG cold energy utilization.

Compared with solutions that require large-scale equipment and industrial chain such as cryogenic pulverization and air separation, the remaining LNG cold energy utilization methods are more flexible, and the demand for geographic location and resource matching is not so great. In theory, it can be combined with the LNG receiving station to realize the recovery and utilization of LNG cold energy without any limitation. However, in addition to cold energy power generation, other cold energy utilization schemes cannot effectively recover the cold energy in the full temperature range of LNG, and some systems such as the air-conditioning systems are also subject to seasonal restrictions and cannot recover LNG cold energy as efficiently as possible.

Japan is the first country in the world to recycle LNG cold energy for power generation. It has rich experience and mature technology. At present, most of the LNG cold energy power plants in operation in the world are in Japan (**Hisazumi, Y. et.al,1998; Miyazaki, T. et.al, 2000**). It is mainly the direct expansion of LNG, indirect Rankine power generation and the combination of the two method (**Karashima, N. 1982**) that is adopted to realize the recovery of LNG cold energy. In fact, the cold energy recovery efficiency of these several power generation methods is not high, and a single cycle cannot achieve the cascade recovery and utilization of LNG cold energy in the full temperature range, which will result in a large amount of waste of cryogenic cold energy. In addition, since the seawater temperature varies greatly with the seasons, in winter, there is a problem of freezing and unusable. Therefore, the power of the LNG cold energy power generation system that uses seawater as the heat source will fluctuate with the seasons. In winter, additional heat source assistance is required to maintain normal operation. The economic comparison of different system proposed for LNG cold energy recovery is presented in the **Table 1**. It can be found that there is no limitation and a high return on investment for the LNG cold energy power generation system, which means it could be promoted on a large scale.

**Table 1** Economic comparison of different system for LNG cold energy recovery

Items	Products	Return on investment	Market sale
Cold storage and cold chain	0.72GJ	21.7%	Limited
Ice and Snow Sports Center	0.72GJ	12.8%	Limited
Cold energy rubber crushing system	0.6t Junked tire	16.7%	Limited
LNG Cold energy air separation system	200kg Liquid Nitrogen 200kg Liquid Oxygen 10kg Liquid Argon	50.0%	Limited
LNG Cold energy ice making system	2t Ice	-	Limited
Air Conditioning refrigeration	0.72GJ	-	Limited
LNG cold energy power generation system	24.3 kW	46.1%	Unlimited
LNG desalination system	1.3ton desalinated seawater	-	Slight limited

In response to the above problems, this paper proposes a system for the comprehensive utilization of LNG cold energy, which can realize the segmented and efficient utilization of LNG cold energy in the full temperature range, and effectively improve the utilization rate of cold energy when the system configuration is more flexible. Moreover, the thermal design of the cold power generation system is carried out, and the one-dimensional design of the turbine is conducted according to the optimized results. The research results are of great significance to engineering guidance.

## 2 Model and assumptions

### 2.1 Introduce of the power generation system based on LNG

According to the scheme proposed above, thermodynamic analysis is conducted on the LNG cold energy power generation system. Considering that the LNG may be likely to be connected to the grid for long-distance transportation in the later stage, this scheme does not recycle and utilize the pressure energy of LNG, but only adopts the simple Rankine cycle to recycle and utilize the cold energy of LNG. However, for a single Rankine cycle, the cold energy of LNG cannot be recycled efficiently in a wide temperature range. Some scholars have proposed three Rankine cycles (In-Hwan Choi et.al, 2013) or even four Rankine cycles (Fenghui Han et.al, 2019) to maximize the cascade recovery of the cold energy of LNG. It seems theoretically feasible for the scheme proposed above to be realized, but there is a lot of difficulty for the actual operation. What is fatal is that the coupling degree between systems is too strong, which is not easy to control, and the construction and maintenance cost is high. Considering the performance, investment cost and engineering application complexity, a new Rankine cycle power generation system based on LNG cold energy recovery and utilization is proposed in this paper. The schematic diagram of the LNG cold power generation system is shown in Figure 1, and the Figure 2 depicts the T-s diagram of the ORC cycle.

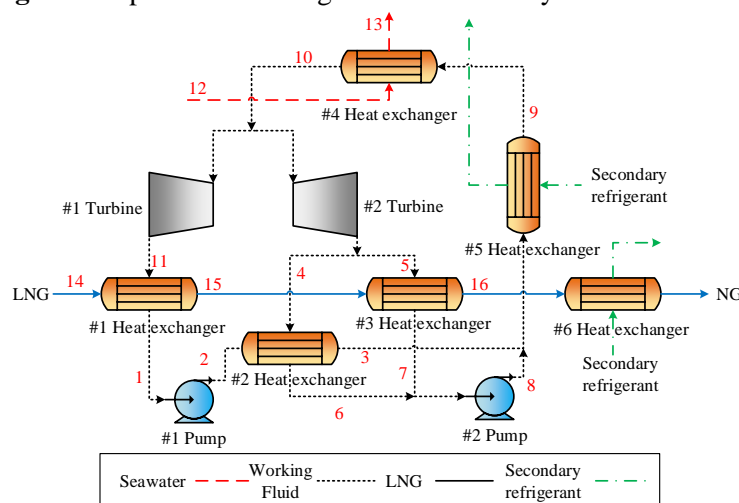


Figure 1 Schematic diagram of the LNG cold energy power generation system

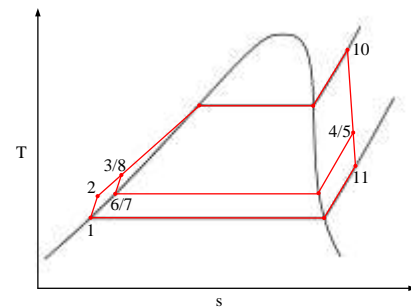


Figure 2 T-s diagram of the LNG cold energy power generation system

It can be seen that after heated by sea water, the working medium is divided into two parts. One part expands to a lower temperature in the #1 turbine and recycles the LNG cold energy with a lower temperature (#1 heat exchanger); the other part expands to a higher temperature in the #2 turbine and further recycles the LNG cold energy (#3 heat exchanger) step by step. In order to make the energy match reasonably and reduce the loss of cold energy, the outlet of #2 turbine is specially diverted, and the pressurized working medium out from the #1 boost pump will be heated by part of the dead gas from #2 turbine. Then the working medium mixture from #2 and #3 heat exchangers is pressurized by #2 booster pump and mixed with the working medium in loop 1 to enter the #5 heat exchanger to exchange heat with coolant that can further recover the cold energy. Finally, the working substance enters #4 heat exchanger and is heated by seawater, then it enters #1 and #2 turbine respectively to do work, thus completing the whole cycle. After being heated twice, the LNG which releases a large amount of cold energy finally enters the #6 heat exchanger and is further heated by secondary refrigerant and finally becomes low-temperature natural gas.

Compared with the traditional Rankine cycle for LNG cold energy recovery, the system proposed in this paper realizes the recovery and application of LNG cold energy through a more reasonable layout and using only one working medium, which greatly improves the recovery rate of cold energy.

### 2.2 Mathematic model

In order to simplify the calculation, some reasonable assumptions are applied in this paper, which are demonstrated as below:

- (1) The system is in steady state without leakage and energy loss.

- (2) The ambient temperature is assumed as 25°C.
- (3) Chemical reaction is ignored in this system
- (4) The turbines and pumps operate with assumed isentropic efficiency.

According to the assumptions, mathematical models could be established, which are shown in Equation (1)-(6).

Power consumption of pump:

$$W_{p1} = G_1(H_2 - H_1) \quad (1)$$

$$W_{p2} = (G_6 + G_7)(H_8 - H_7) \quad (2)$$

Power capacity of turbine

$$W_{t1} = G_{11}(H_{10} - H_{11}) \quad (3)$$

$$W_{t2} = (G_4 + G_5)(H_{10} - H_5) \quad (4)$$

Cold energy recovery rate:

$$\eta = \frac{(W_{t1} + W_{t2} - W_{p1} - W_{p2})}{G_{LNG}(H_{out} - H_{in})} \quad (5)$$

Cold exergy recovery rate:

$$\eta_{ex} = \frac{(W_{t1} + W_{t2} - W_{p1} - W_{p2})}{G_{LNG}(E_{out} - E_{in})} \quad (6)$$

### 2.3 One-dimensional design model of the axial turbine

Considering that the mass flow rate of the working fluid is large, axial turbine is selected as the expansion device, which adopts one-dimensional design. The main mathematical model is shown as follows (Equations (7)-(25)). During the turbine performance analysis, the loss of the wheel circumference including nozzle loss, rotor blade loss, residual velocity loss, annular cascade loss, impeller friction loss and partial inlet loss (blast loss and arc end loss) are mainly considered (Xinjun Wang et al, 2014). Figure 3 shows the thermodynamics process in the turbine stage, where the subscript *s* represents the isentropic state, and the inlet of the turbine considers the steam throttle. Figure 4 shows the speed triangle of the stage, and the main design process of this paper is carried out according to the speed triangle of the stage. The flow chart of one-dimensional design of axial turbine is demonstrated in Figure 5. By adjusting the evaporation pressure of the system, the initial condition of the turbine calculation is changed, thus the final turbine isentropic efficiency after iteration could be higher than 80%, which is consistent with initial assumptions.

Total isentropic enthalpy drop:  $H_s^* = H_{0'} - H_{0s}$  (7)

The isentropic enthalpy drop at each stage:  $H_{si}^* = \lambda_i H_s^*$  (8)

Ideal absolute velocity outside the nozzle:  $c_{1s} = \sqrt{2(1-\Omega)H_{s1}^*}$  (9)

Absolute velocity outside the nozzle:  $c_1 = \phi c_{1s}$  (10)

Peripheral speed:  $u = \frac{\pi d_m n}{60}$  (11)

Relative velocity outside the nozzle:  $w_1 = \sqrt{c_1^2 + u^2 - 2c_1 u \cos \alpha_1}$  (12)

Relative flow angle outside the nozzle:  $\beta_1 = \arccos\left(\frac{c_1 \cos \alpha_1 - u}{w_1}\right)$  (13)

Relative velocity outside the rotor blade:  $w_2 = \phi \sqrt{w_1^2 + 2\Omega H_{s1}^*}$  (14)

Absolute velocity outside the rotor blade:  $c_2 = \sqrt{w_2^2 + u^2 - 2w_2 u \cos \beta_2}$  (15)

Absolute flow angle outside the rotor blade:  $\alpha_2 = \arccos\left(\frac{w_2 \cos \beta_2 - u}{c_2}\right)$  (16)

Height of the nozzle  $l_1 = G / (\rho_1 \pi d_m e c_1 \sin \alpha_1)$  (17)

Height of the rotor blade  $l_2 = G / (\rho_2 \pi d_m e c_2 \sin \alpha_2)$  (18)

The wheel periphery power  $W_{u,i} = Gu(c_1 \cos \alpha_1 - w_2 \cos \beta_2)$  (19)

Stage power  $W_{i,i} = W_{u,i} - G(\xi_f + \xi_v + \xi_{en} + \xi_l)H_{si}^*$  (20)

Friction loss coefficient  $\xi_f = k_1 u^3 d_m^2 \rho / (GH_{si}^*)$  (21)

Windage loss coefficient  $\xi_v = 2.1k_2(1-e)d_m l_2^{1.5} u^3 \rho / (GH_{si}^*)$  (22)

The arc end loss coefficient  $\xi_{en} = 0.135B_2 l_2 n u \eta_u / (d_m l_1 e c_{1s} \sin \alpha_1 \sqrt{1-\Omega})$  (23)

Cascade loss coefficient  $\xi_l = 0.7(l_2 / d_m)^2$  (24)

Relative internal efficiency of stage  $\eta_i = \sum_{i=1} W_{i,i} / GH_s^*$  (25)

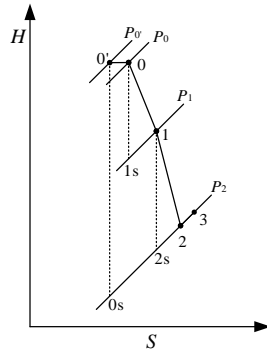


Figure 3 Thermal process curve of turbine stage

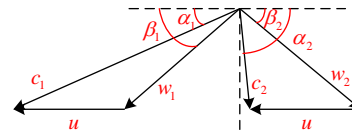


Figure 4 speed triangle of turbine stage

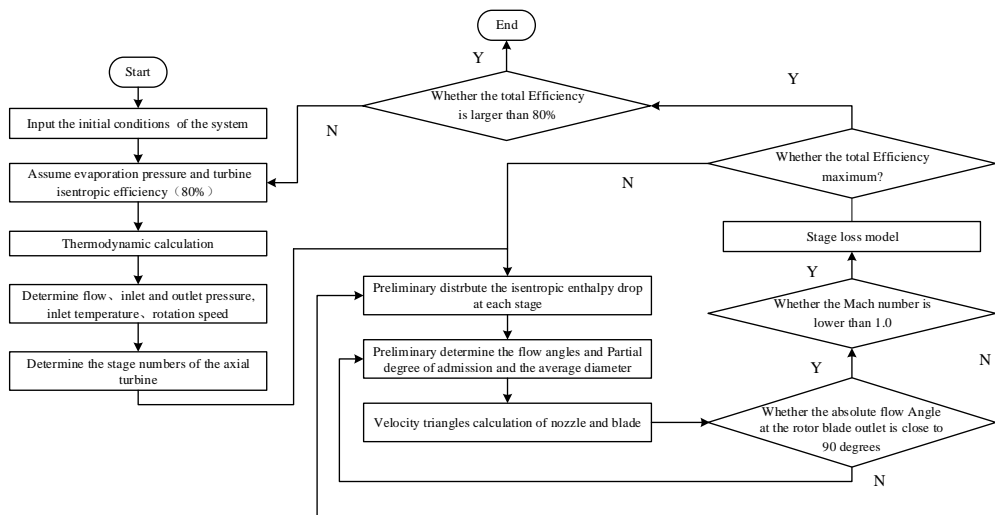


Figure 5 Flow Chart of one-dimensional design of axial turbine

### 3 Results and discussion

Taking both the cost of the working medium and its applicable scope into consideration, R125 (ODP=0, GWP=2800) is final selected as the working fluid in the power generation system. All the physical properties of working fluid and LNG are based on the database of NIST REFPROP10.0 (Lemmon, E.W et.al, 2018).

Figure 6 and Figure 7 present the system net power, thermal efficiency, exergy efficiency variation with the turbine inlet pressure and turbine inlet temperature, respectively. It can be reserved that both the thermal efficiency and the exergy efficiency of the system is increased with the evaporation pressure  $p_{10}$ , while the system net power decreases. However, with the growth of turbine inlet temperature  $t_{10}$ , all the system performance improved.

Actually, it could not be indefinitely enhanced of the system performance. Without extra heat source, the maximum turbine inlet temperature should be lower than ambient temperature because of the heat transfer temperature drop. Moreover, it is necessary to let the steam superheat to avoid entering the two-phase region, which is benefit of the turbine operation. Besides, the LNG out of the system may be

further utilized, so it is necessary to supplied for the downstream users as much as possible. Consequently, the system efficiency of the system needs to be a priority.

Taking both the above factors and the calculation convenience into account, the final turbine inlet pressure and temperature are 1000 kPa and 15 °C, respectively. On the basis of that, the parameters of each state point of the power generation system could be obtained, shown in the Table 2. According to the results, the cold energy recovery rate of the LNG power generation system is 22.74%, while the cold exergy recovery rate of the LNG power generation system is 33.24%, and the maximum net power of the system is 4616.89 kW.

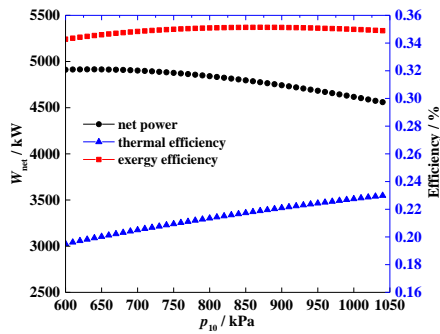


Figure 6 System performance variation with  $p_{10}$

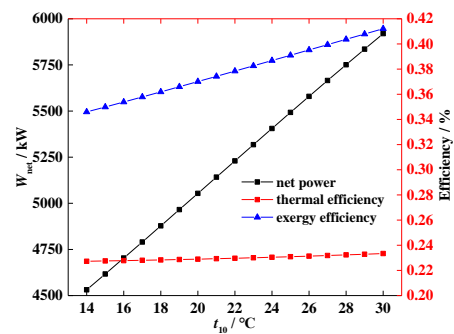


Figure 7 System performance variation with  $t_{10}$

Table 2 Results of state point in the LNG cold energy power generation system

State point	$G$ (kg·s <sup>-1</sup> )	$P$ (kPa)	$T$ (K)	$H$ (kJ·kg <sup>-1</sup> )	$s$ (J·kg <sup>-1</sup> ·K <sup>-1</sup> )	$E$ (kJ·kg <sup>-1</sup> )
1	89	30	203.11	119.32	661.80	70.497
2	89	1000	203.50	120.08	662.55	71.036
3	89	1000	237.95	158.13	835.15	57.625
4	20.559	180	247.89	322.15	1527.36	15.268
5	69.541	180	247.89	322.15	1527.36	15.268
6	20.559	180	237.53	157.43	834.57	57.102
7	69.541	180	237.53	157.43	834.57	57.102
8	90.1	1000	237.95	158.13	835.15	57.625
9	179.1	1000	263.15	187.70	953.22	51.995
10	179.1	1000	293.15	345.42	1507.89	44.338
11	89	30	207.59	297.67	1539.79	-12.916
12	6709.36	500	298.15	357.18	1589.74	31.697
13	6709.36	500	293.15	352.97	1575.50	31.732
14	50.26	10000	111.15	-15.34	-24.01	998.813
15	50.26	9800	202.59	300.50	2023.03	704.334
16	50.26	9600	242.81	528.43	3047.30	626.872

The thermodynamic boundaries of turbine #1 and turbine #2 were obtained from the results mentioned in Table 2, as shown in the table below:

Table 3 Boundary conditions of the turbine design

	#1 Turbine	#2 Turbine
Mass flow rate(kg·s <sup>-1</sup> )	89	90.1
Turbine inlet pressure (MPa)	1	1
Turbine inlet temperature (°C)	20	20
Discharge pressure (MPa)	0.03	0.18
Rotation speed (rpm)	3000	3000
Working fluid	R125	R125

Table 4 Design results of #1 turbine

	C1	2	3	4	5
--	----	---	---	---	---

Average diameter (mm)	770	780	800	840	880
Ideal speed ratio of stage	0.456	0.448	0.428	0.417	0.455
Absolute flow angle at nozzle outlet (°)	18.026	18.026	18.026	18.026	13.978
Absolute flow angle at rotor outlet (°)	94.257	91.375	84.428	80.962	98.511
Mach number at nozzle outlet	0.980	0.997	1.072	1.172	1.151
Height of the nozzle (mm)	27.0	45.0	76.9	143.6	374.7
The blade root diameter (mm)	743.0	735.0	723.1	696.4	505.3
Height of the rotor blade (mm)	30.5	50.2	83.3	153.2	386.1
Stage power (kW)	646.763	704.645	820.173	942.691	838.305
Stage isentropic efficiency (%)	82.636	84.663	85.414	84.656	66.945

**Table 5** Design results of #2 turbine

	C1	2	3
Average diameter (mm)	770	780	800
Ideal speed ratio of stage	0.456	0.448	0.441
Absolute flow angle at nozzle outlet (°)	18.026	18.026	18.026
Absolute flow angle at rotor outlet (°)	94.257	91.375	88.903
Mach number at nozzle outlet	0.980	0.997	1.039
Height of the nozzle (mm)	27.3	45.6	77.4
The blade root diameter (mm)	754.57	754.57	757.28
Height of the rotor blade (mm)	30.9	50.9	85.4
Stage power (kW)	655.2834	713.6417	714.436
Stage isentropic efficiency (%)	82.70225	84.6969	78.08956

According to the results in **Table 4** and **Table 5**, the designed #1 turbine adopts five-stage arrangement, its designed power is 3952.577 kW, and the isentropic efficiency is 81.86%. The #2 turbine adopts three-stage arrangement, with a design power of 2083.361 kW and an isentropic efficiency of 82.51%. It can be seen that the efficiency of the actual one-dimensional turbine design is more than 80%, which indicates a better prospect of the whole system could be achieved for engineering application.

#### 4 CONCLUSIONS

A newly designed system is proposed to comprehensively recover and utilize the cold energy of liquid natural gas (LNG). Thermodynamic analysis of the power generation system in the comprehensive system is conducted, and the one-dimensional design is carried out for the two turbines in the power generation system. The main conclusions can be drawn as below:

- (1) With the growth of turbine inlet pressure and temperature, both the system thermal and exergy efficiency increase, and the net power output declines under the former condition while improving in the later case.
- (2) The cold energy recovery rate of the LNG power generation system is 22.74%, while the cold exergy recovery rate of the LNG power generation system is 33.24%.
- (3) The designed power of the two turbines are separately 3952.577 kW and 2083.361 kW, While the isentropic efficiencies of the two turbines are 81.86% and 82.51%, respectively, which is close to the value estimated in the thermodynamic calculation.

#### NOMENCLATURE

B	Width of rotor cascade	(mm)
c	absolute velocity	(m/s)
d	diameter	(mm)
e	partial degree of admission	
E	specific exergy	(kJ/kg)
G	mass flow rate	(kg/s)
H	specific enthalpy	(kJ/kg)

k	empirical coefficient	
l	length	(mm)
n	rotation speed	(r/min)
P	pressure	(kPa)
T	temperature	(K)
s	specific entropy	(J/(kg·K))
u	peripheral velocity	(m/s)
w	relative velocity	(m/s)
W	power	(kW)
$\alpha$	absolute flow angle	( $^{\circ}$ )
$\beta$	relative flow angle	( $^{\circ}$ )
$\phi$	nozzle velocity coefficient	
$\varphi$	rotor velocity coefficient	
$\xi$	loss coefficient	
$\lambda$	enthalpy drop coefficient	
$\Omega$	degree of reaction	

## REFERENCES

- Global, B.P., Worldwide, B.P., 2011. BP Energy Outlook 2030. London, UK.
- Soldo, B., 2012. Forecasting natural gas consumption. Applied energy 92, 26-37.
- Ikoku, C.U., 1980. Natural gas engineering: a systems approach.
- Wong, W., 1994. LNG power recovery. Proceedings of the Institution of Mechanical Engineers, Part A: Journal of Power and Energy 208(1), 3-12.
- Dubinsky, Z.V.Y., Stambler, N., 1996. Marine pollution and coral reefs. Global change biology 2(6), 511-526.
- Hirakawa, S., Kosugi, K., 1981. Utilization of LNG cold. International Journal of Refrigeration 4(1), 17-21.
- He, T., Chong, Z.R., Zheng, J., Ju, Y., Linga, P., 2019. LNG cold energy utilization: Prospects and challenges. Energy 170, 557-568.
- Bao, J., Yuan, T., Zhang, L., Zhang, N., Zhang, X., He, G., 2019. Comparative study of liquefied natural gas (LNG) cold energy power generation systems in series and parallel. Energy Conversion and Management 184, 107-126.
- Ma, G., Lu, H., Cui, G., Huang, K., 2018. Multi-stage Rankine cycle (MSRC) model for LNG cold-energy power generation system. Energy 165, 673-688.
- Li, C., Liu, J., Zheng, S., Chen, X., Li, J., Zeng, Z., 2019. Performance analysis of an improved power generation system utilizing the cold energy of LNG and solar energy. Applied Thermal Engineering 159, 113937.
- Hisazumi, Y., Yamasaki, Y., Sugiyama, S., 1998. Proposal for a high efficiency LNG power-generation system utilizing waste heat from the combined cycle. Applied Energy 60(3), 169-182.
- Miyazaki, T., Kang, Y.T., Akisawa, A., Kashiwagi, T., 2000. A combined power cycle using refuse incineration and LNG cold energy. Energy 25(7), 639-655.
- Karashima, N., Akutsu, T., Development of LNG cryogenic power generation plant, 1982. CONF-820814- ed. The Tokyo Electric Power Co., Inc., Tokyo.
- Choi, I.-H., Lee, S., Seo, Y., Chang, D., 2013. Analysis and optimization of cascade Rankine cycle for liquefied natural gas cold energy recovery. Energy 61, 179-195.
- Han, F., Wang, Z., Ji, Y., Li, W., Sunden, B., 2019. Energy analysis and multi-objective optimization of waste heat and cold energy recovery process in LNG-fueled vessels based on a triple organic Rankine cycle. Energy Conversion and Management 195, 561-572.
- Lemmon, E.W., Bell, I.H., Huber, M.L., McLinden, M.O., 2018. NIST Standard Reference Database 23: Reference Fluid Thermodynamic and Transport Properties-REFPROP, Version 10.0, National Institute of Standards and Technology. Standard Reference Data Program, Gaithersburg.

Wang, X.J, Li, L, Song, L.M, Li, J., 2014. Primary Theory of Steam Turbine. Xi'an Jiaotong University Press., Xi'an